TRANSIENT MOTION OF AN INDUSTRIAL MIXER WITH ELASTICALLY SUSPENDED WORK HEAD

Venelin Jivkov[1] – Rosen Mitrev[2][*]

[1]Department of Theory of Mechanisms and Machines, Faculty of Industrial Technology, Technical University of Sofia, 1797 Sofia, Bulgaria
[2]Department of Logistics Engineering, Material Handling and Construction Machines, Mechanical Engineering Faculty, Technical University of Sofia, 1797 Sofia, Bulgaria

ARTICLE INFO	Abstract:
	This paper investigates the transient behavior of a novel design of an industrial mixer incorporating additional work head movement. In contrast to conventional models, this mixer consists of an elastic torsion bar with its longitudinal axis oriented orthogonally to the main drive shaft axis. Using the elastic torsion bar to hang the workhead adds an additional degree of freedom, greatly improving the mixing of fluids or powders. The motion of the electro-mechanical device was simulated using a system of nonlinear differential equations that consider the dynamic characteristics of the driving electric motor, as derived from the theorem for the rate of change of angular momentum. A numerical analysis was carried out to study the transient processes in the system under different working conditions. Finally, a constrained multiobjective optimization was performed to identify the optimal design variable values that minimize the force and power characteristics of the mixer.

1 Introduction

Over the past two decades, there has been an increasing demand for industrial equipment in the chemical, food, pharmaceutical and construction industries to produce superior quality products. One crucial aspect of manufacturing processes involves the mixing of powder or liquid substances. For this purpose, various types of equipment are employed, including reactors, agitators, homogenizers, mixers, emulsifiers, and other devices that utilize pure rotation, spatial, or epicyclic movement in their work heads [1] - [3]. These devices can operate in continuous/batch mode or stationary/start-stop mode. Despite the availability of a wide range of equipment models in the market, researchers and manufacturers in this field are consistently focused on developing new models that offer improved performance. For example, a recently patented design [4] proposes suspending the mixer work head from a torsion bar positioned orthogonally to the longitudinal axis of the main drive shaft. This unique configuration lets the work head tilt during rotation, resulting in an increased mixing radius driven by centrifugal forces. Furthermore, the additional rotation of the work head enhances the liquid mixture.

The mechanical structure of mixers is classified as rotor systems, which is a extensively researched field. Several books and monographs delve into the theoretical foundations of rotor system mechanics [5]-[8]. Researchers have investigated various rotor system structures to evaluate their dynamic behavior. In many cases, the dynamic processes of rotor systems are non-linear and involve significant deformations and eccentricity, leading to multiple dynamic regimes characterized by bifurcations and instability [9]. In [10] is analyzed a two-rotor system with an incorrect arrangement of the rotor axes and discovered that a specific frequency spectrum component could be used for axis shift diagnosis. Similarly, the paper [11] investigated a rotating coupled-rotor system with four disks incorporating an inter-shaft bearing, considering disk eccentricity. The authors developed a finite element method (FEM) model of the rotor system using

---

[*] Corresponding author
E-mail address: rosenm@tu-sofia.bg

_____

commercial software and confirmed its validity through experiments. The study conducted in [12] performed modal analysis of a high-speed rotor system comprised of an impeller and a turbine supported by two bearings, using both experimental and numerical methods. The results demonstrated a substantial agreement between the computed and experimentally obtained natural frequencies. In [13], a structurally less complex rotor system consisting of an elastic shaft, a rotor and two non-linear supports was examined. The assumed mode method and the harmonic balance method were used to obtain the nonlinear frequency response of the system. Various researchers have conducted theoretical and experimental studies on systems subjected to both limited [14] and unlimited excitation [15], [16]. Some studies have focused on optimizing rotor systems, such as the work presented in [17], where a multi-objective genetic algorithm was employed to optimize weight and stability in a simple bearing-rotor system. In [18] is studied the instability induced by the airflow excitation force (Alford force) in a Jeffcott rotor and optimized the stiffness of the supports and shaft diameters to significantly improve the stability of the rotor system. Last, in [19] is employed a genetic optimization method to optimize the design of an eccentric rotor system with a squeeze film damper, resulting in a 15% improvement in system stability and reduced vibration amplitude.

The differential equations of motion for rotor systems are typically derived using well-established methods such as Lagrange [20], Newton-Euler [21], [22], or the theorem for the rate of change of angular momentum [23]. Analytical solutions for these equations are rare, and numerical techniques are commonly employed instead [24]. In certain scenarios, approximate methods such as the small parameter method, harmonic balance, harmonic linearization, asymptotic methods, or T-transformation [25], [26] prove to be suitable alternatives. Gubanov and Cortelezzi [27] emphasize the importance of determining the optimal mechanical configuration and operating conditions for industrial mixers. They propose integrating dynamic models of industrial mixer structures with existing experimental studies [1], theoretical analyses [28], and simulation studies [29] to further support the development of optimal mixer designs. This integrated approach offers the potential to expedite the design process and facilitate the creation of competitive designs within shorter timeframes.

The present study aims to investigate the transient modes exhibited by the novel mixer design presented in reference [4], which features a work head suspended from a torsion bar, oriented orthogonally to the longitudinal axis of the main drive shaft. By employing a multi-criteria optimization technique, the study seeks to identify the optimal values of design variables that will minimize an objective function comprising the force and power characteristics of the system.

2 Mathematical modeling of the system

2.1 *Principle of operation of the mixer*

Figure 1 portrays the fundamental elements of the mixer, which encompass an elastic torsion bar positioned orthogonally to the longitudinal axis of the main drive shaft. These elements are: 1) An electric motor with a conical rotor; 2) A conical friction brake; 3) An elastic coupling; 4) A work head featuring a displaced mass center; and 5) An elastic torsion bar. The mixer can operate either continuously or in a sequence of start-stop cycles, with each cycle enduring about 6 to 7 seconds. During each cycle, the mixer accelerates to the maximum angular velocity of the motor, operates at that velocity, and then undergoes forced deceleration due to the motor's electric supply being severed and subsequent automatic activation of the conical brake.

The electric motor rotates the work head at an angular velocity $\dot{\varphi}_2$. The center of mass of the work head undergoes a radial displacement of ε and a vertical displacement of e, as illustrated in Figure 4. This displacement results in the generation of a centrifugal force, which induces the twisting of the elastic torsion bar and causes the work head to tilt at an angle α relative to the vertical axis. Improved mixer performance can be achieved through the expansion of the mixing radius, additional movement of the head, and the implementation of a series of start-stop cycles.Figure 2 presents the mixer's kinematic scheme and adopted coordinate systems for describing the relative motion of the links: the inertial coordinate system $x_0y_0z_0$, the coordinate system $x_1y_1z_1$ fixed to the motor's rotor, and the coordinate system $x_2y_2z_2$ fixed to the work head. Figure 3 shows the mechanical system dynamic model, which illustrates the system's elastic, damping, torque, and inertial properties.
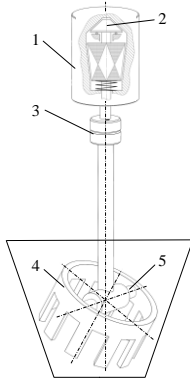
Figure 1. Basic parts.   *Figure 2. Kinematic scheme.*   *Figure 3. Dynamic model.*
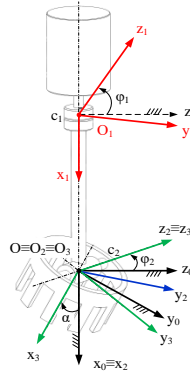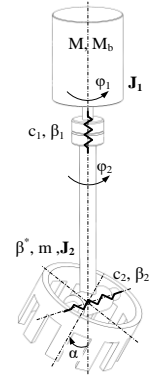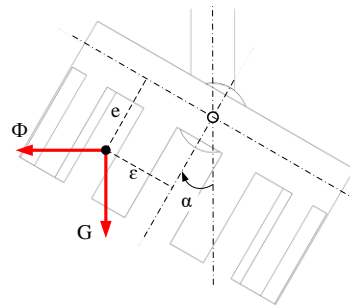
Figure 4. Side view of the work head.

2.2 Equations of motion

The following notations are used in Figure 2 and Figure 3: φ_1, φ_2 are the angles of rotation of axes z_1 and z_2 around the immovable axis x_0 - $\prec z_1 z_0 = \varphi_1$, $\prec z_2 z_0 = \varphi_2$; α is the angle of rotation around the axis z_2 - $\prec x_2 x_3 \equiv \prec y_2 y_3 = \alpha$; c_1, c_2 and β_1, β_2 are elasto-damping coefficients of the elastic elements; $\mathbf{J}_1$, $\mathbf{J}_2$ are the tensors of mass-moments of inertia of the electric motor and the work head, correspondingly:

$$\mathbf{J}_1 = \begin{bmatrix} A_1 & 0 & 0 \\ 0 & B_1 & 0 \\ 0 & 0 & B_1 \end{bmatrix}, \ \mathbf{J}_2 = \begin{bmatrix} A_2 & -F_2 & -E_2 \\ -F_2 & B_2 & -D_2 \\ -E_2 & -D_2 & B_2 \end{bmatrix}$$

β^* is the dissipation coefficient, which represents the resistance of the hydraulic fluid against the rotation of the work head; T is the electric motor time constant; M is the electric motor's torque; $M^* = \beta^* \dot{\varphi}_2^2$ is the hydraulic resistance moment, applied to the mixer's work head; m is the mass of the work head; $\Phi = m\varepsilon\dot{\varphi}_2^2$ is the inertial force (see Figure 4); M_b is the torque, developed by the cone brake.

The rotation matrices between the adjacent coordinate systems are (see Figure 2):

$$\mathbf{R}_0^1 = \begin{bmatrix} 1 & 0 & 0 \\ 0 & \cos\varphi_1 & -\sin\varphi_1 \\ 0 & \sin\varphi_1 & \cos\varphi_1 \end{bmatrix}, \ \mathbf{R}_0^2 = \begin{bmatrix} 1 & 0 & 0 \\ 0 & \cos\varphi_2 & -\sin\varphi_2 \\ 0 & \sin\varphi_2 & \cos\varphi_2 \end{bmatrix}, \ \mathbf{R}_2^3 = \begin{bmatrix} \cos\alpha & -\sin\alpha & 0 \\ \sin\alpha & \cos\alpha & 0 \\ 0 & 0 & 1 \end{bmatrix}$$

After the linearization is performed, assuming that the values of the angle α and the relative angle $\Delta\varphi = \varphi_1 - \varphi_2$ are small, one obtains the following vectors for the bodies i absolute angular velocities $\boldsymbol{\omega}_i$:

$$\boldsymbol{\omega}_1 = \begin{bmatrix} \dot\varphi_1 \\ 0 \\ 0 \end{bmatrix}, \; \boldsymbol{\omega}_2 = \begin{bmatrix} \dot\varphi_2 \\ 0 \\ 0 \end{bmatrix}, \; \boldsymbol{\omega}_3 = \begin{bmatrix} \dot\varphi_2 \\ 0 \\ \dot\alpha \end{bmatrix}$$

Applying the theorem for the rate of change of the angular momentum [23] $\mathbf{K}_i$ (i=1,2,3) along the three generalized coordinates φ_1, φ_2, and α, from Figure 2 follows the system of equations:

$$\begin{cases} \dot{\mathbf{K}}_i + \mathbf{M}_i = 0, (i = 1,2,3) \\ T\dot{M} + M = a - b\dot\varphi_1 \end{cases} \tag{1}$$

where $\mathbf{K}_i = \mathbf{J}_i\boldsymbol{\omega}_i$ is the angular momentum (i=1,2,3);

$$\mathbf{M}_1 = \mathbf{M}_{12} - \mathbf{M}_d, \; \mathbf{M}_{12} = \begin{bmatrix} c_1(\varphi_1 - \varphi_2) + \beta_1(\dot\varphi_1 - \dot\varphi_2) \\ 0 \\ 0 \end{bmatrix}, \; \mathbf{M}_d = \begin{bmatrix} M \\ 0 \\ 0 \end{bmatrix};$$

$$\mathbf{M}_2 = -\mathbf{M}_{12} + \mathbf{M}^r + \mathbf{M}^*, \; \mathbf{M}^* = \begin{bmatrix} \beta^*\dot\varphi_2^2 \\ 0 \\ 0 \end{bmatrix}, \; \mathbf{M}^r = \begin{bmatrix} E_2\dot\varphi_2^2\alpha + 2F_2\dot\varphi_2\dot\alpha \\ -F_2\dot\varphi_2^2\alpha - 2E_2\dot\varphi_2\alpha \\ (A_2 - B_2)\dot\varphi_2^2 - F_2\dot\varphi_2^2 \end{bmatrix};$$

$$\mathbf{M}_3 = -\mathbf{M}^r + \mathbf{M}_{23} - \mathbf{M}_\Phi + \mathbf{M}_G, \; \mathbf{M}_{23} = \begin{bmatrix} 0 \\ 0 \\ c_2\alpha + \beta_2\dot\alpha \end{bmatrix}, \; \mathbf{M}_\Phi = \begin{bmatrix} 0 \\ 0 \\ M_\Phi \end{bmatrix}, \; \mathbf{M}_G = \begin{bmatrix} 0 \\ 0 \\ M_G \end{bmatrix};$$

$$M_\Phi = \frac{1}{2}m\dot\varphi_2^2\left(2e\varepsilon\cos(2\alpha) + (e^2 - \varepsilon^2)\sin(2\alpha)\right), M_G = mg(\varepsilon\cos\alpha + e\sin\alpha);$$

The second scalar equation in (1) represents the dynamic characteristic [14] of the electric direct current motor with a time constant T, which value depends on the ratio of active and inductive resistance in its windings, typically $0.01 \le T \le 0.35$. By a and b are denoted the coefficients of the static motor's characteristic. After performing needed mathematical operations in (1) and some simplifications, the system of differential equations is represented as:

$$\begin{cases} A_1\ddot\varphi_1 + c_1(\varphi_1 - \varphi_2) + \beta_1(\dot\varphi_1 - \dot\varphi_2) = M \\ A_2\ddot\varphi_2 - E_2\ddot\alpha - c_1(\varphi_1 - \varphi_2) - \beta_1(\dot\varphi_1 - \dot\varphi_2) + \beta^*\dot\varphi_2^2 + E_2\dot\varphi_2^2\alpha + 2F\dot\varphi_2\dot\alpha = 0 \\ B_2\ddot\alpha - E_2\ddot\varphi_2 + c_2\alpha + \beta_2\dot\alpha - (B_2 - A_2)\dot\varphi_2^2\alpha - F_2\dot\varphi_2^2 = M_\Phi - M_G \\ T\dot{M} + M = a - b\dot\varphi_1 \end{cases} \tag{2}$$

The system (2) solution is carried out after the presentation as:

$$\begin{cases} \ddot{\mathbf{q}} = \mathbf{A}^{-1}(\mathbf{Q} - \mathbf{B}\dot{\mathbf{q}} - \mathbf{C}\mathbf{q} - \mathbf{N}) \\ \dot{M} = \dfrac{a - b\dot\varphi_1 - M}{T} \end{cases} \tag{3}$$

where the following notations are used:

$$\mathbf{q} = \begin{bmatrix} \varphi_1 \\ \varphi_2 \\ \alpha \end{bmatrix}, \ \mathbf{A} = \begin{bmatrix} A_1 & 0 & 0 \\ 0 & A_2 & -E_2 \\ 0 & -E_2 & B_2 \end{bmatrix}, \ \mathbf{B} = \begin{bmatrix} \beta_1 & -\beta_1 & 0 \\ -\beta_1 & \beta_1 & 0 \\ 0 & 0 & \beta_2 \end{bmatrix}, \ \mathbf{C} = \begin{bmatrix} c_1 & -c_1 & 0 \\ -c_1 & c_1 & 0 \\ 0 & 0 & c_2 \end{bmatrix},$$

$$\mathbf{N} = \begin{bmatrix} 0 \\ \beta^* \dot{\varphi}_2^2 + E_2 \dot{\varphi}_2^2 \alpha + 2F \dot{\varphi}_2 \dot{\alpha} \\ -(B_2 - A_2) \dot{\varphi}_2^2 \alpha - F_2 \dot{\varphi}_2^2 \end{bmatrix}, \ \mathbf{Q} = \begin{bmatrix} M \\ 0 \\ M_\Phi - M_G \end{bmatrix}$$

2.3 Numerical study of the transient processes

The system of differential equations (3) is highly nonlinear and stiff, thus numerical solutions are obtained using specialized numerical methods [24]. Figures 5 to 13 display the solutions of the system (3), obtained under the initial conditions (4). The numerical values of the parameters used are presented in Table 1, where t_f represents the simulation duration.

Table 1. Numerical values of the parameters.

Parameter	Numerical value
c_1, [Nm]	40000
c_2, [Nm]	2500
A_1, [kg.m^2]	0.4
B_1, [kg.m^2]	0.2
A_2, [kg.m^2]	5
B_2, [kg.m^2]	0.2
E_2, [kg.m^2]	0.8
F_2, [kg.m^2]	0.3
a, [Nm]	420
b, [Nms]	4.7
β_1, [Nms]	0.4
β_2, [Nms]	0.4
ε, [m]	0.0005
e, [m]	0.05
m, [kg]	120
t_f, [s]	3

$$\varphi_1(0) = \varphi_2(0) = \alpha(0) = 0$$
$$\dot{\varphi}_1(0) = \dot{\varphi}_2(0) = \dot{\alpha}(0) = 0 \qquad (4)$$
$$M(0) = 0$$

In Figure 5 ÷ Figure 13 are shown solutions for output characteristics of the studied electro-mechanical system.
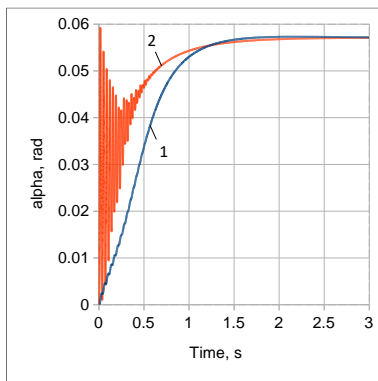
Figure 5. Angle α.
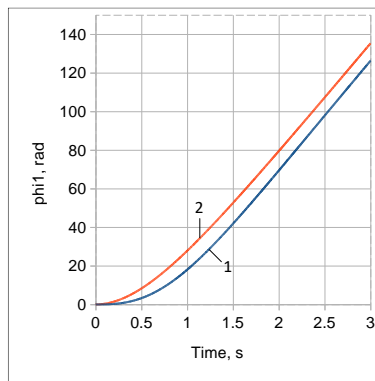
Figure 6. Angle φ_1.
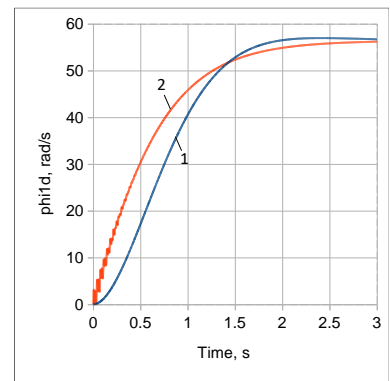
Figure 7. Angular velocity.
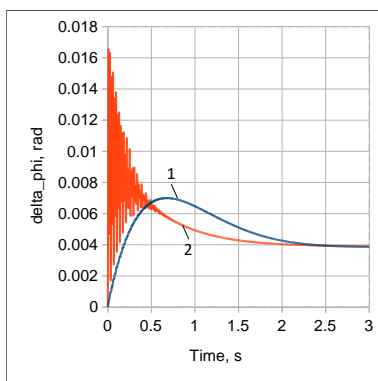
Figure 8. Relative angle $\Delta\varphi$.
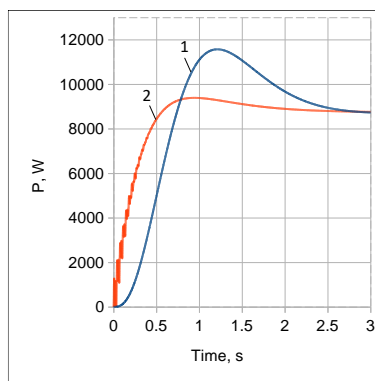
Figure 9. Motor power P.
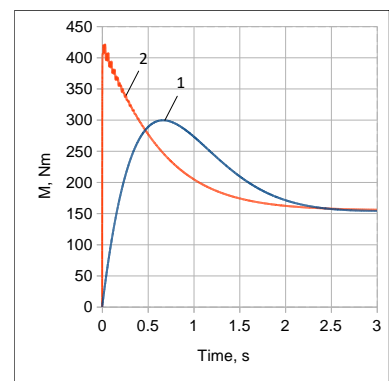
Figure 10. Motor torque M.
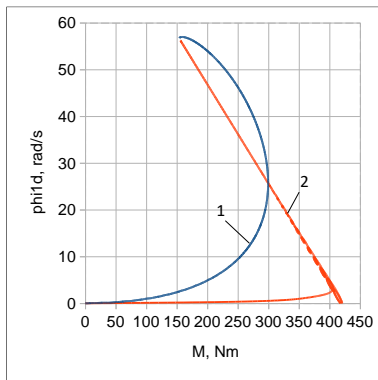
Figure 11. Motor characteristics $\dot{\varphi}_1(M)$.
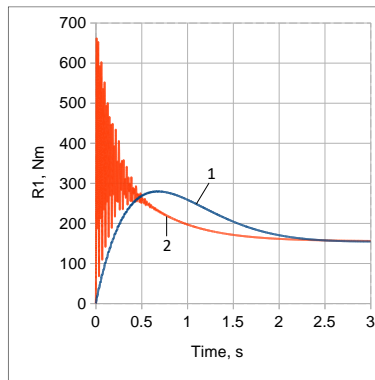
Figure 12. Torque R_1 in the coupling.
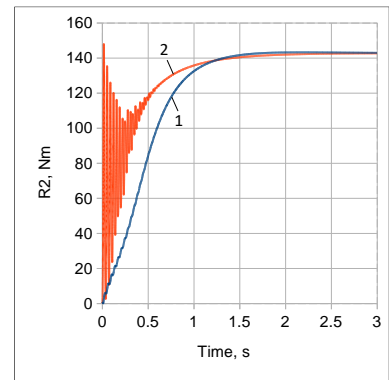
Figure 13. Torque R_2 in the torsion bar.
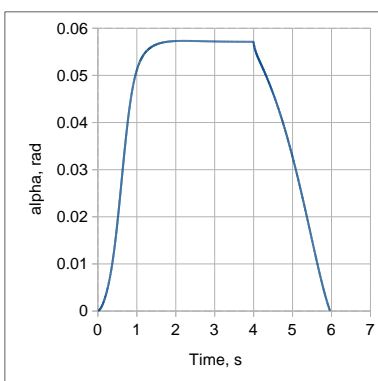
Figure 14. Angle α.
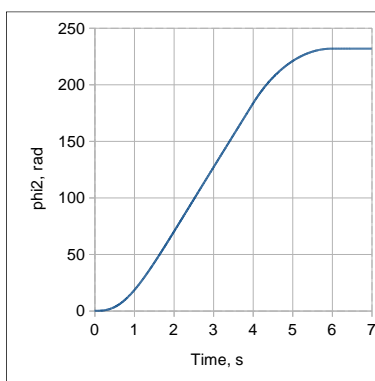
Figure 15. Angle φ_2.
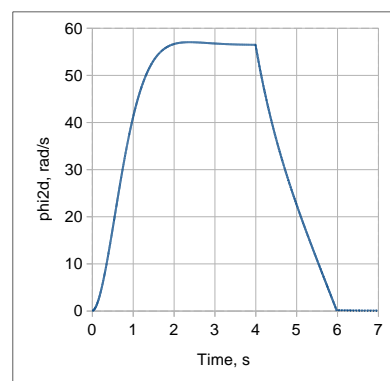
Figure 16. Angular velocity $\dot{\varphi}_2$.

_____

For every output characteristic, two solutions have been obtained - one with the maximum time constant value of $T = 0.35$ s, denoted in figures as position 1, and the other with the minimum time constant value of $T = 0.001$ s, denoted as position 2. Figure 5 illustrates the effect of T value on the transient process of α, which is the rotation of the work head around the torsion bar's longitudinal axis. For a small T value, the steady-state value of α is attained in about 0.5 s, and the transient process is accompanied by damped oscillations, unlike the case with a large T value, where the steady-state value of α is reached in about one second with the absence of oscillations. Damping oscillations are also seen in the graphs of the moments of the elastic coupling, as in Figure 12, and in the torsion bar, as in Figure 13. Figure 12 demonstrates that a small value of the motor time constant results in a characteristic closely resembling the static one, with a straight-line shape. Increasing the value of T results in a change in the type of characteristic. Figures 14, 15, and 16 present the transient modes of α, φ_2, and $\dot{\varphi}_2$ obtained by applying a braking torque $M_b = 100$ Nm to the motor's rotor at time $t=4$ s, after reaching a steady state. The complete start-stop cycle, including acceleration and deceleration periods, takes 6 to 7 seconds. One can observe that the decrease in the characteristic graphs is nearly linear during the deceleration period.

3   Multicriteria optimization of the dynamic system

The presence of multiple geometrical, inertial, elastic, and damping parameters necessitates the identification of their optimal combination to enhance specific system characteristics while ensuring compliance with technological and design constraints. The studied system multicriteria optimization problem [30], [31] is formulated as a weighted linear combination [32], [33] of the following objectives: 1) The maximum value of the motor power squared; 2) The square of the torque in the elastic coupling; and 3) The square of the torque in the torsion bar.

$$\textbf{min} \quad Z = k_1 \max P^2 + k_2 \max R_1^2 + k_3 \max R_2^2 \tag{5}$$

where P is the electric motor power:

$$P = M\dot{\varphi}_1 \tag{6}$$

R_1 is the torque in the elastic coupling:

$$R_1 = c_1\left(\varphi_1 - \varphi_2\right) + \beta_1\left(\dot{\varphi}_1 - \dot{\varphi}_2\right) \tag{7}$$

R_2 is the torque in the torsion bar:

$$R_2 = c_2\alpha + \beta_2\dot{\alpha} \tag{8}$$

$k_i\,(i=1,2,3)$ represents the weighting for the criteria*;*

Minimization of objective function (4) should be performed with the following constraints:
- Constraints on generalized coordinate values **q** imposed by the system of differential equations (2), solved under initial conditions (3);
- A constraint imposed by the value $\left[\alpha\right]$ of the angle α at the end of the simulation time interval $t = \left[0, t_F\right]$

$$\alpha\left(t_F\right) = \left[\alpha\right] \tag{9}$$

This constraint is introduced to define the required value of the tilt angle of the working head;
- An interval constraint imposed on the angular speed of the motor, defined by technological requirements of the mixing process:

_____

$$\dot{\varphi}_1^{\min} \le \dot{\varphi}_1 \le \dot{\varphi}_1^{\max} \tag{10}$$

where $\dot{\varphi}_1^{\min}$ and $\dot{\varphi}_1^{\max}$ are the lower and upper limits of the angular velocity.

To account for the presence of constraints, the objective function is extended with two additional penalty terms U_1 and U_2, defined using the method of penalty functions [32]:

$$\mathbf{min} \quad Z = k_1 \max P^2 + k_2 \max R_1^2 + k_3 \max R_2^2 + k_4 U_1 + k_5 U_2 \tag{11}$$

where:

$$U_1 = \max\left(0, \dot{\varphi}_1^{\min} - \dot{\varphi}_1\right)^2 + \max\left(0, \dot{\varphi}_1 - \dot{\varphi}_1^{\max}\right)^2 \tag{12}$$

$$U_2 = \left(\alpha\left(t_F\right) - [\alpha]\right)^2 \tag{13}$$

and k_4 and k_5 are the corresponding weights.

Classic or modern metaheuristic methods [34] are appropriate for addressing the optimization problem. In this instance, the optimization was conducted using the Powell method [35]. Based on the relative significance of the individual components within the objective function (11) and employing a trial and error approach, the following values of the weighting coefficients in (11) were chosen: k_1=500, k_2=1, k_3=1, k_4=500×10³, k_5=1×10¹².
From a technological process perspective, it is advantageous that the value of $[\alpha]$ is close to $\pi/2$. The additional analysis shows that the numerical error made due to the linearization of the system of differential equations is negligibly small just up to values around $[\alpha] = 0.1$, which value is accepted in the constraint (9).

Table 2 shows the accepted intervals of the design variables and the optimum values reached. Table 1 illustrates the initial values for the design variables. The initial value of the objective function (11) is 2.015×10^9, and the final value is 1.331×10^7.

Table. 2 Design variables intervals and their optimal values.

Design variable	Lower limit	Upper limit	Optimal value
c_1, [Nm]	30000	50000	49287.3
c_2, [Nm]	2000	3000	2000
A_1, [kg.m²]	0.3	0.5	0.442
B_1, [kg.m²]	0.1	0.3	0.2
A_2, [kg.m²]	3	7	3.05
B_2, [kg.m²]	0.1	0.3	0.147
E_2, [kg.m²]	0.6	1	0.6
F_2, [kg.m²]	0.2	0.4	0.293
a, [Nm]	200	600	416.3
b, [Nms]	0.5	10	0.901
T, [s]	0.1	0.3	0.230
β_1, [Nms]	0.2	0.5	0.2
β_2, [Nms]	0.2	0.5	0.2
ε, [m]	0.0002	0.002	0.00052
e, [m]	0.001	0.2	0.05
m, [kg]	100	140	123.12

Figure 17 – Figure 22 shows graphs of selected mechanical system output characteristics. Within each Figure, position 1 shows the plot at the values of the initial parameters, and position 2 is the plot subsequent to optimization. One can see from Figure 20 and Figure 21 that the constraints for α and $\dot{\varphi}_1$ are satisfied.

_____
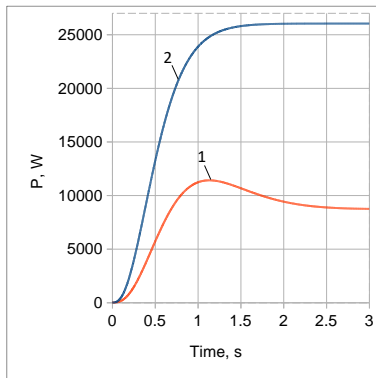
Figure 17. Motor power P.
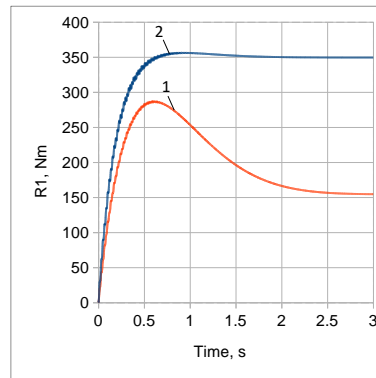
Figure 18. Torque in the coupling R_1.
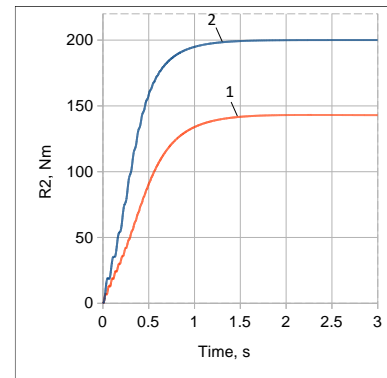
Figure 19. Torque in the torsion bar R_2.
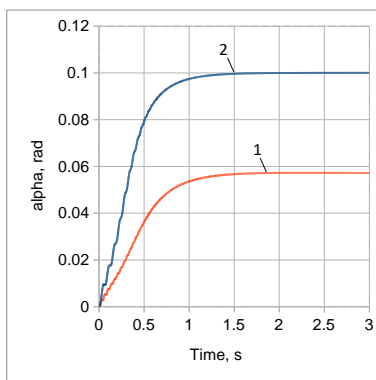
Figure 20. Angle α.
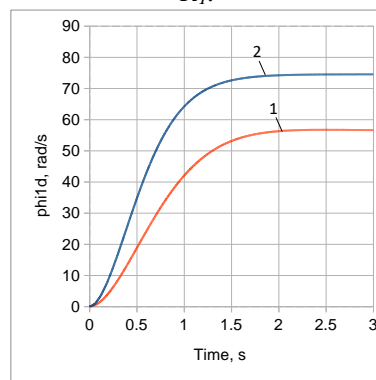
Figure 21. Angular velocity $\dot{\varphi}_1$.
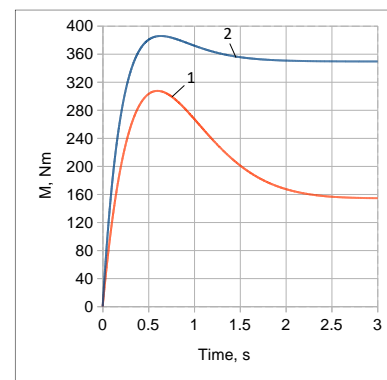
Figure 22. Motor torque M.

4   Conclusion

The results of the dynamic analysis and multi-objective optimization of the innovative mixer present compelling evidence for several significant findings. Firstly, in the continuous operation mode of the mixer, the work head exhibits reduced movements around the *z*-axis of the torsion bar, resulting in reduced efficiency compared to the favored start-stop modes. Start-stop modes can be readily achieved through straightforward technical methodologies. Secondly, small motor time constant values lead to substantial positive gradients of the transient process, leading to damped oscillations around the mean-integral values of the torques in the coupling and the torsion bar. On the other hand, large time constant values significantly alter the torque characteristics of the electric motor. Thirdly, optimizing the mixer's design variables made it possible to determine optimal values of the system parameters, leading to the minimization of the torques in the elastic coupling and torsion bar, as well as the electric motor power. Optimization considers that linearization introduces some error in the mathematical model, which explains why the tilting angle of the working head is limited by a constraint. The new elastic suspension developed for the work head is simple to implement and does not require significant investment, making it an attractive option for competitive industrial applications. Our future aim is to investigate the mathematical model of a mixer, incorporating an extra degree of freedom into its design, thereby enhancing its functionality and output characteristics.

References

[1]   E. Paul, V. Atiemo-Obeng, and S. Kresta, "Handbook of industrial mixing. Science and practice," Wiley-Interscience, New Jersey, 2004.

[2]   D. Karaivanov, S. Bekzhanov, and B. Saktaganov, "Torque method investigation of wolfrom gear trains," *Engineering Review*, Vol. 43, No. 1, 2023.

[3]   S. Troha , Ž. Vrcan , D. Karaivanov , and M. Isametova, "The selection of optimal reversible two-speed planetary gear trains for machine tool gearboxes," *Facta Universitatis series: Mechanical Engineering*, Vol. 18, No 1, pp. 121– 134, 2020, https://doi.org/10.22190/FUME191129013T

[4]   V. Jivkov, K. Stoichkov, and N. Nikolov, "Industrial mixer-homogenizer with additional oscillating movement of the mixing head," Patent Agency, Bulgaria, 28.06.2023, № BG/U/2023/5778 (pending).

[5]   R. Tiwari, "Rotor Systems: Analysis and Identification," CRC Press, Taylor & Francis Group 2018.

[6]   M. Lalane, and G. Feritas, "Rotor's Dynamics," Prediction in Engineering 2-nd Edition New York, Wiley, 1997.

[7]   W. J. Chen, and E. J. Gunter, "Introduction to Dynamics of rotor-bearing systems," Trafford publishing, 2007.

[8]   E. Kramer, "Dynamics of Rotors and Foundation," Berlin, Germany, Springer Verlag, 1993.

[9]   H. P. Phadatare, and B. Pratiher, "Nonlinear modeling, dynamics, and chaos in a large deflection model of a rotor–disk–bearing system under geometric eccentricity and mass unbalance," *Acta Mechanica*, 231(3), 907–928, 2019, doi:10.1007/s00707-019-02559-9

[10]   Z. Li, J. Li, and M. Li, "Nonlinear dynamics of unsymmetrical rotor-bearing system with fault of parallel misalignment," *Advances in Mechanical Engineering*, 10(5), 2018, doi:10.1177/1687814018772908

[11]   N. Wang, D. Jiang, and H. Xu, "Dynamic characteristics analysis of a dual-rotor system with inter-shaft bearing," *Proceedings of the Institution of Mechanical Engineers, Part G: Journal of Aerospace Engineering*, 233(3):1147-1158, 2019. doi:10.1177/0954410017748969

[12]   M. H. Jalali, M. Ghayour, S. Ziaei-Rad, and B. Shahriari, "Dynamic analysis of a high speed rotor-bearing system," *Measurement*, Vol. 53, Pages 1-9, 2014, https://doi.org/10.1016/j.measurement.2014.03.010.

[13]   M. K. Al-Solihat, and K. Behdinan, "Force transmissibility and frequency response of a flexible shaft–disk rotor supported by a nonlinear suspension system," *International Journal of Nonlinear Mechanics*, Vol. 124, 103501, 2020, https://doi.org/10.1016/j.ijnonlinmec.2020.103501.

[14]   V. Jivkov, "Some Singularity in Rotor's Systems with Limited Excitation," *Comptes Rendus de L'Academie Bulgare des Sciences,* Tome 69 №3, 2016.

[15]   V. Jivkov, and E. Zahariev, "Stability and non-stationary vibrations of the Rotor in elasto-viscous field," *Int. Journ. Mechanics Based Design of Structures and Machines*, 42(1), pp.35 – 55, 2014, https://doi.org/10.1080/15397734.2013.814545

[16]   V. Jivkov, and E. Zahariev, "Non-stationary phenomena of rotating multibody systems," Comptes rendus de l'Académie Bulgare des Sciences, vol. 68, no. 4, Apr. 2015, pp. 505+

[17]   X. Kuang, G.- Luo, and F. Wang, "Multiobjective rotor dynamics optimization of the plain bearing-rotor system," *Vibroengineering Procedia*, Vol. 20, pp. 278–282, Oct. 2018, https://doi.org/10.21595/vp.2018.20289

[18]   Y. Fu, and F. Wang, "Instability threshold analysis and optimization of a rotor system considering the Alford force," *Vibroengineering Procedia*, Vol. 43, pp. 82–89, Jun. 2022, https://doi.org/10.21595/vp.2022.22716

[19]   R. CholUk, Z. ZhunHyok, C. ChungHyok, Z. Qiang, R. JuYong, and K. CholHyok, "Optimization Design Analysis of the Eccentric Rotor System with SFD," *J. Vib. Eng. Technol*, 10, 751–765, 2022, https://doi.org/10.1007/s42417-021-00406-7

[20]   D. Sado, J. Freundlich, and A. Bobrowska, "Chaotic vibration of an autoparametrical system with the spherical pendulum", *Journal of Theoretical and Applied Mechanics (Poland)*, 55, pp. 779-786, 2017.

[21]   V. Jovanović, D. Marinković, D. Janošević, and N. Petrović, "Influential Factors in the Loading of the Axial Bearing of the Slewing Platform Drive in Hydraulic Excavators," *Tehnički vjesnik,* Vol. 30, No. 1, pp.158-168, 2023, https://doi.org/10.17559/TV-20220425205603

[22]   V. Jovanović, D. Janošević, and J. Pavlović, "Analysis of the influence of the digging position on the loading of the slewing platform bearing in hydraulic excavators," Facta Universitatis series: Mechanical Engineering, Vol. 19, No 4, pp. 705 – 718, 2021, https://doi.org/10.22190/FUME190225020J

[23]   H. Baruh, "Analytical dynamics," WCB/McGraw-Hill, 1999.

[24]   I. Kožar, M. Plovanić, and T. Sulovsky, "Derivation matrix in mechanics – data approach," *Engineering*

_____

Review, vol. 43, No. 1, 2023.

[25]   M. Kolovsky, "Dynamics of Machines," Moscow, Russia, (in Russian), 1989

[26]   G. Puhov, "Taylor transformations and their applications in electrical Engineering and Electronics," Kiev, 1978.

[27]   O. Gubanov, and L. Cortelezzi, "Towards the design of an optimal mixer," Journal of Fluid Mechanics, 651, 27, 2010, doi:10.1017/s0022112009993806

[28]   J. Zhang, S. Xu, and W. Li, "High shear mixers: A review of typical applications and studies on power draw, flow pattern, energy dissipation and transfer properties," *Chemical Engineering and Processing: Process Intensification*, Vol. 57–58, pp. 25-41, 2012, https://doi.org/10.1016/j.cep.2012.04.004.

[29]   A.P. Herman, J. Gan, and A. Yu, "GPU-based DEM simulation for scale-up of bladed mixers," *Powder Technology*, vol. 382, pp.300-317, 2021, doi:10.1016/j.powtec.2020.12.045

[30]   S. H. Zolfani , M. Yazdani , D. Pamucar, and P. Zarate, "A VIKOR and TOPSIS focused reanalysis of the MADM methods based on logarithmic normalization," Facta Universitatis series: Mechanical Engineering, Vol. 18, No 3, pp. 341-355, 2020, https://doi.org/10.22190/FUME191129016Z

[31]   S. Chatterjee and S. Chakraborty, "A Multi-criteria decision making approach for 3D printer nozzle material selection," *Rep Mech Eng*, 4(1), 62–79, 2023, https://doi.org/10.31181/rme040121042023c

[32]   R. L. Rardin, "Optimization in operations research,". Second edition. Pearson, 2017

[33]   J. Stefanović-Marinović, Ž. Vrcan, S. Troha, and M. Milovančević, "Optimization of Two-Speed Planetary Gearbox With Brakes on Single Shafts," *Rep Mech Eng*, 3, 94-107, 2022

[34]   M. Franulović, K. Marković , and A. Trajkovski, "Calibration of material models for the human cervical spine ligament behaviour using a genetic algorithm," Facta Universitatis series: Mechanical Engineering, Vol. 19, No 4, pp. 751– 765, 2021, https://doi.org/10.22190/FUME201029023F

[35]   M.J.D. Powell, "An efficient method for finding the minimum of a function of several variables without calculating derivatives,"*Computer Journal,* 7 (2): 155–162, 1964, doi:10.1093/comjnl/7.2.155. hdl:10338.dmlcz/103029